

This item is the archived peer-reviewed author-version of:

Recent developments in fullfield thickness measurements of the human eardrum

Reference:

van der Jeught Sam, Dirckx Joris.- Recent developments in fullfield thickness measurements of the human eardrum
Journal of otology & rhinology - ISSN 2324-8785 - 6:2(2017)
Full text (Publisher's DOI): <http://dx.doi.org/doi:10.4172/2324-8785.1000312>

Recent developments in full-field thickness measurements of the human eardrum

S. Van der Jeught^{1,*}, J. Dirckx¹

¹Laboratory of Biomedical Physics, Department of Physics, University of Antwerp. Groenenborgerlaan 171, B-2020 Antwerp, Belgium

*corresponding author: sam.vanderjeught@uantwerpen.be

Abstract:

Recently, we published several full-field human tympanic membrane data sets that were obtained using a modified high-resolution optical coherence tomography setup¹. In this short communication letter, we provide an overview of the active research fields in which these data have been used or in which human tympanic membrane thickness measurements play an instrumental role. These applications include finite element modeling of the middle ear system, medical diagnosis of middle ear pathology and the design of tympanic membrane grafts.

¹ Van der Jeught, S. *et al.* Full-field thickness distribution of human tympanic membrane obtained with optical coherence tomography. *J. Assoc. Res. Otolaryngol.* **14**, 483–94 (2013).

1. Introduction:

The human tympanic membrane (TM) or eardrum is a conically shaped membrane that separates the external ear canal from the middle ear (ME) cavity. In humans, the tympanic membrane's surface area ($\sim 50\text{-}70\text{ mm}^2$) is rather large in comparison to its average thickness range ($\sim 50\text{-}150\text{ }\mu\text{m}$). This imposes several important limitations to potential imaging techniques that can be used to scan its thickness distribution. On the one hand, the depth resolution has to be sufficiently high to detect any local thickness variations. On the other hand, the system needs to be able to capture the entire TM in its field-of-view whilst at the same time maintaining a sufficiently high lateral resolution when scanning the membrane from edge to edge. In order to obtain full-field thickness data of human eardrums, considerable effort has been made. Magnetic resonance imaging (MRI) of the human middle ear² allows the orientation and geometry of the tympanic membrane to be observed clearly, but is unable to resolve its subtle thickness variations. Due to the low X-ray absorption of soft tissue, general micro-scale X-ray computed tomography (μCT) images of the TM have limited contrast quality, preventing the technique from producing a detailed thickness distribution of the tympanic membrane³. Applying phosphotungstic acid staining to the samples increases the X-ray absorption of soft tissue, which results in images with higher contrast⁴, but the chemical treatment of the sample may cause thickness and shape aberrations in the TM. The optical sectioning ability of confocal microscopy (CM) was used to produce a thickness map based on a set of high-resolution measurements along several lines of the TM⁵. However, the typical height of the human TM ($\sim 1.5\text{-}2\text{ mm}$) greatly exceeds the working distance of confocal microscopes, requiring the sample to be flattened out in order to maintain depth resolution. In addition, the field of view of CM is several times smaller than the surface area of the typical human TM, inducing possible stitching errors in the construction of the full data map.

In optical coherence tomography (OCT) images, the axial and lateral resolutions are decoupled from one another, allowing OCT setups to maintain a high resolution across the entire sample volume in all three dimensions. The added benefits of OCT imaging include its non-invasiveness, non-destructiveness and absence of ionizing radiation, and, in principal, the possibility to implement the probing head into a surgical endoscope. This combination of properties makes OCT a highly suitable imaging modality for in-situ and in vivo measurement of human eardrum thickness. In a recent study¹, we modified a large-volume optical coherence tomography setup to obtain full-field thickness distributions, three-dimensional surface models and general morphological data of six human tympanic membranes.

In the next section, we will briefly discuss the custom OCT setup and the post-processing techniques that were employed to gather the raw TM thickness data. We review these thickness data, we discuss general thickness trends of the human eardrum and we describe

the construction of an average human eardrum model. In section 3, we explore a variety of applications and fields of study in which accurate and full-field human thickness data are indispensable. Finally, we conclude the letter in section 4.

2. Optical coherence tomography measurements of the human tympanic membrane

2.1 Human tympanic membranes

Five tympanic membranes (TM1-5) were harvested from human cadavers and were made available by the Temporal Bone Foundation - Brussels. In order to comply with the regulations of the National Health Service (NHS), UK, blinded samples were employed. Before commencement of the measurements, these temporal bones were examined for irregularities under a microscope to ensure that they possessed normal otological middle ears.

2.2 Large-volume OCT setup

The employed measurement setup was developed at the Applied Optics Group at the University of Kent, Canterbury. Optical sections through the eardrum were made using a customized large-volume OCT system⁶, equipped with a wide-angle galvo-scanning unit. An enlarged detail of the scanning configuration is included in Figure 1. The probing beam crosses the collimation-condensing lens L1 at a location determined by the tilting angles of the two scanning mirrors S_x and S_y , each independently capable of creating transversal B-scans (labeled B_x and B_y , respectively) in mutually perpendicular directions. By scanning the beam along the X-axis using the line-scanning mirror S_x , whilst keeping the frame scanning mirror S_y fixed, a B-scan cross section is produced in the XZ-plane with coordinate Y determined by the tilt of the frame scanning mirror. Repeating the process for multiple adjacent Y-values, a stack of B-scan images is acquired. Typically, the line scanning mirror rotates at a higher frequency than the frame scanning mirror. Note the difference in curvature between the two transversal scans B_x and B_y of the same flat mirror (FM). As the two scanning mirrors reflect the probing beam consecutively, their respective beam reflecting points each have a different optical path length to the surface of the sample.

Because of the wide scanning angles of the rotating mirrors, the resulting measurements suffer from non-linear geometric distortion artifacts in which the degree of distortion is determined by the maximum angles over which the mirrors rotate. Therefore, a set of coordinate transformations were applied in post-processing to correct for these geometric distortion artifacts. The accuracy of the large-volume OCT setup was validated to maintain a resolution of $<15 \mu\text{m}$ within the sample, both axially and transversally, within a large imaging volume of $12.35 \times 10.13 \times 2.36 \text{ mm}^3$.

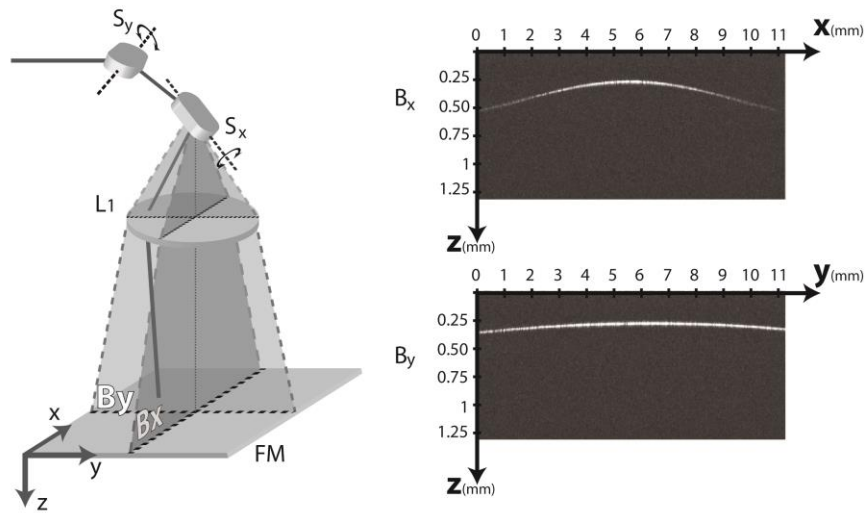


Figure 1: Enlarged detail of the scanning unit in the object arm in the OCT setup. Rotating one of the two scanning mirrors (S_x or S_y) whilst keeping the other one fixed, produces a B-scan (B_x or B_y) perpendicular to its respective axis of rotation. By measuring a flat mirror using the employed setup, the imposed geometric distortion artifacts could be corrected for in post-processing.

After geometric distortion correction, the transversal OCT scans were segmented into binary labels. From these cross-sections, local thickness data and general morphological and geometric properties of the membranes were gathered. A selection of numerical properties of TM1-5 is included in table 1. Full models and two-dimensional thickness maps are available for download¹ at the website of the Laboratory of Biomedical Physics, Antwerp.

	Inf-Sup (mm)	Ant-Post (mm)	Surf. area (mm ²)	Apex (mm)	$\langle T \rangle$ (μm)
TM1	8.86	8.11	67.95	1.72	97.01
TM2	7.73	8.36	58.76	1.49	79.56
TM3	7.96	7.55	49.84	1.51	84.28
TM4	8.21	8.73	61.55	1.75	88.98
TM5	8.05	8.47	60.44	1.53	83.55

Table 1: Numerical values of several geometric features of the human TM models that were extracted from OCT data. Columns 1 and 2: inferior-superior and anterior-posterior length of the TM, respectively. Column 3: surface area of the lateral side of the membrane. Column 4: the apex of the membrane, determined as the shortest distance between the XY -plane

¹ www.uantwerpen.be/bimef > downloads > Middle & inner ear models

and the umbo. Column 5: average values of the thickness distribution measured at the pars tensa of the membrane, excluding the manubrium.

2.3 Thickness data of human tympanic membrane

Although considerable differences in absolute thickness were observed between the 5 tympanic membranes that were measured, their relative thickness profiles did contain several similar features. In general, thickness increases steeply from 40-75 μm in the central region between annulus and manubrium to 110-160 μm when moving over a small distance of 1-2 mm from the central region towards either the peripheral rim of the pars tensa or towards the manubrium. In addition, 4 out of 5 membranes contained a local thickening in the antero-inferior quadrant, between the umbo and the edge of the pars tensa.

These general thickness trends have prompted us to construct a virtual 'averaged' model of the human tympanic membrane. The full-field thickness data of TM1-5 were combined into a single model of the human eardrum by projecting their respective thickness distributions onto the same averaged surface shape. It should be noted that the absolute thickness values of the membranes were not altered during this process. They were merely repositioned onto the same surface shape and resampled on the same grid by 2D interpolation. In this way, a virtual membrane was constructed that represents the averaged thickness map of the five healthy eardrums that were included in the study. This average TM model (TMA) is depicted in 2D and in 3D in the graphical summary of the post-processing pipeline in Figure 2. In general, the averaged model has a thin central region of 50-70 μm , a local thickening in the antero-inferior quadrant of 80-100 μm , and a steep increase in thickness near the peripheral rim of the pars tensa and towards the manubrium up to 120-140 μm . Although the inter-specimen variability between different human tympanic membranes is large and there is no such thing as an "average human eardrum", quantification of these similar trends and incorporation into a single model could provide more insight into the fundamental anatomy of the human eardrum and enables modelers to employ more accurate and representative distributions of mass in their finite element models of the human TM.

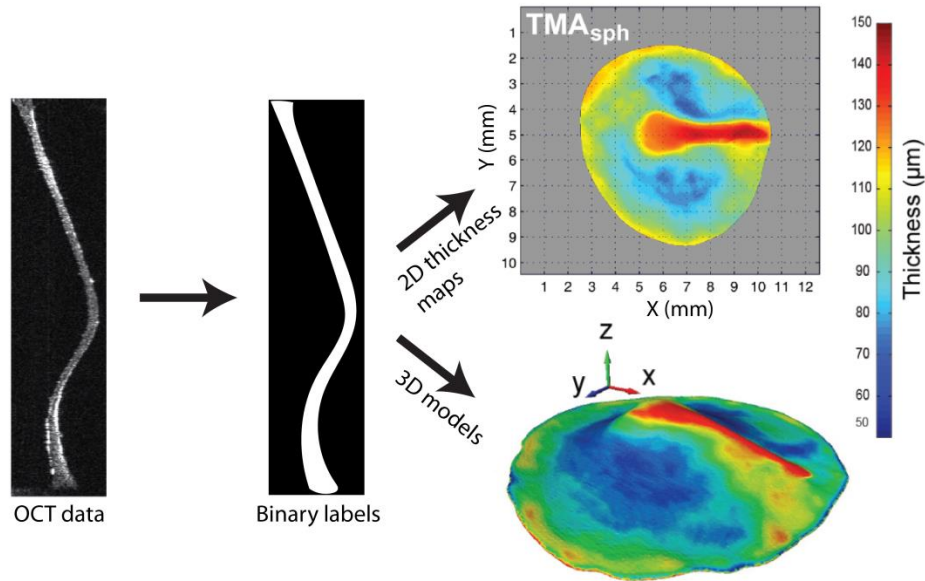


Figure 2: Post-processing pipeline. Raw 2D OCT data are segmented into binary files and combined into 2D thickness maps and 3D models.

3. Recent developments in tympanic membrane thickness metrology and its application in finite element modeling and otoscopy

Although there was a general consensus on the inhomogeneous mass distribution in different locations on the TM, the lack of accurate full-field thickness data caused the earliest applications of finite element modeling (FEM) in hearing research to employ single thickness values across the entire membrane⁷. With the advent of high-resolution non-invasive depth scanning techniques such as OCT, and with the increase in computational processing power, more and more sophisticated models of the middle ear are being developed^{8,9}. Combination of the earlier presented full-field TM thickness data with measurements of the sound-induced motion of the TM surface and with cone-beam CT measurements of the incudo-malleal (IM) joint has led to detailed finite element models that allowed more accurate estimation of the viscoelastic properties of the TM¹⁰ and high-precision morphometric analysis of the human IM complex¹¹.

As TM thickness is an important precursor for impending or manifested otitis media, recent efforts have been made to implement optical coherence tomography sectioning into a portable, hand-held otoscopic probe. Both *ex-vivo*¹² and *in-vivo*^{13,14} studies were performed and demonstrated a clear correlation between increased thickness and otitis media. As there is a large inter-specimen variation in TM thickness between healthy patients, it should be noted that multiple measurements on a single membrane may be required in order to construct a thickness baseline and to detect aberrant sites on the TM.

Therefore, Hubler et al. implemented a high-speed segmentation algorithm that is able to determine the upper and lower boundaries of the TM. This way, the local thickness can be calculated in real-time. Quantitative thickness measurements may provide healthcare practitioners with an objective biomarker to diagnose acute and chronic otitis media in patients that otherwise show no conclusive symptoms when inspected during regular otoscopy.

Finally, recent advances in multi-material 3D printing have enabled the fabrication of biomimetic TM grafts with micrometer scale accuracy^{15,16}. The artificially constructed grafts were found to better resist deformation than the most commonly used temporalis fascia grafts and eliminated the need for additional skin incisions when harvesting the fascia. Furthermore, the composite grafts exhibit similar acoustic properties and spatial displacement patterns as those found in fascia and cadaveric grafts. Although this microscale 3D printing technique is still in its early phase of development and additional microstructure fine-tuning and mechanical testing is necessary, it does provide a first step towards reproducible replacement of damaged or diseased tympanic membranes. Nevertheless, given the complex non-uniform thickness distribution of the human tympanic membrane, increased precision of the 3D eardrum model architecture will greatly benefit the acoustic performance of the grafts, especially at high frequencies.

4. Conclusion

Full-field tympanic membrane thickness models of five healthy human ears were presented and made available online. Local thickness distribution is an important parameter in the construction of artificial eardrum grafts and finite element models of middle ear functioning. It may be used as a biomarker in the clinical office as an indicator of existing or impending (chronic) otitis media.

Acknowledgment

The authors thank the Research Foundation—Flanders (FWO) for their financial support and Prof. Podoleanu and the Applied Optics Group at the University of Kent, Canterbury, for their collaboration in obtaining the OCT data sets.

1. Van der Jeught, S. *et al.* Full-field thickness distribution of human tympanic membrane obtained with optical coherence tomography. *J. Assoc. Res. Otolaryngol.* **14**, 483–94 (2013).
2. Lin, T., Yu, J. & Chen, C. Magnetic Resonance Imaging of the In-vivo Human Tympanic Membrane. 166–171 (2010).
3. Buytaert, J. A. N., Salih, W. H. M., Dierick, M., Jacobs, P. & Dirckx, J. J. J. Realistic 3D computer model of the gerbil middle ear, featuring accurate morphology of bone and soft tissue structures. *JARO - J. Assoc. Res. Otolaryngol.* **12**, 681–696 (2011).
4. Metscher, B. D. MicroCT for comparative morphology: simple staining methods allow high-contrast 3D imaging of diverse non-mineralized animal tissues. *BMC Physiol.* **9**, 11 (2009).
5. Kuypers, L. C., Decraemer, W. F. & Dirckx, J. J. J. Thickness distribution of fresh and preserved human eardrums measured with confocal microscopy. *Otol. Neurotol.* **27**, 256–264 (2006).
6. Van der Jeught, S., Buytaert, J. a N., Bradu, A., Podoleanu, A. G. & Dirckx, J. J. J. Real-time correction of geometric distortion artefacts in large-volume optical coherence tomography. *Meas. Sci. Technol.* **24**, 57001 (2013).
7. Vollandri, G., Di Puccio, F., Forte, P. & Carmignani, C. Biomechanics of the tympanic membrane. *Journal of Biomechanics* **44**, 1219–1236 (2011).
8. Lee, D. & Ahn, T.-S. Statistical calibration of a finite element model for human middle ear. *J. Mech. Sci. Technol.* **29**, 2803–2815 (2015).
9. Rohani, S. A., Ghomashchi, S., Agrawal, S. K. & Ladak, H. M. Estimation of the Young's modulus of the human pars tensa using in-situ pressurization and inverse finite-element analysis. *Hear. Res.* (2017). doi:10.1016/j.heares.2017.01.002
10. De Greef, D. *et al.* Viscoelastic properties of the human tympanic membrane studied with stroboscopic holography and finite element modeling. *Hear. Res.* **312**, 69–80 (2014).
11. Soons, J. A. M. *et al.* 3D morphometric analysis of the human incudomalleal complex using clinical cone-beam CT. *Hear. Res.* 1–10 (2016). doi:10.1016/j.heares.2016.01.014
12. Kirsten, L. *et al.* Doppler optical coherence tomography as a promising tool for detecting fluid in the human middle ear. **2**, 443–447 (2016).
13. MacDougall, D., Farrell, J., Brown, J., Bance, M. & Adamson, R. Long-range, wide-field swept-source optical coherence tomography with GPU accelerated digital lock-in Doppler vibrography for real-time, in vivo middle ear diagnostics. *Biomed. Opt. Express* **7**, 4621–4635 (2016).

14. Hubler, Z. *et al.* Real-time automated thickness measurement of the in vivo human tympanic membrane using optical coherence tomography. *Quant. Imaging Med. Surg.* **5**, 69–77 (2015).
15. Kozin, E. D. *et al.* Design, fabrication, and in vitro testing of novel three-dimensionally printed tympanic membrane grafts. *Hear. Res.* 1–13 (2015).
doi:10.1016/j.heares.2016.03.005
16. Crafts, T. D. *et al.* Three-Dimensional Printing and Its Applications in Otorhinolaryngology-Head and Neck Surgery. *Otolaryngol. -- Head Neck Surg.* (2016).
doi:10.1177/0194599816678372